Supplementary Information

Harvesting of Light Energy by Iridium(III) Complexes on a Clay Surface

Kenji Tamura,[a] Akihiko Yamagishi,[b] Takafumi Kitazawa,[b,c] and Hisako Sato,[d]*

[a] National Institute of Materials Science, Tsukuba 305-0044, Japan
[b] Department of Chemistry, Toho University, Funabashi, Chiba 274-851,Japan
[c] Research Center For Materials with Integrated Properties, Toho University, Funabashi, Chiba 274-851,Japan
[d] Department of Chemistry, Graduate School of Science and Engineering, Ehime University, Matsuyama 790-8577, Japan, sato.hisako.my@ehime-u.ac.jp

Contnets

1. ^{1}H NMR and mass spectra

$[Ir(dfppy)_2(C_1\text{-bpy})]ClO_4$

^{1}H NMR (chloroform-*d*, 400MHz, 25 °C): δ 9.59 (s, 2H), 8.33 (d, J = 8.0 Hz, 2H), 7.84 (t, J = 7.2 Hz, 2H), 7.73 (d, J = 5.6 Hz, 2H), 7.52 (d, J = 4.2 Hz, 2H), 7.25 (d, J = 5.6 Hz, 2H), 7.10 (dd, J = 6.0, 6.0 Hz, 2H), 6.58 (t, J = 9.8 Hz, 2H), 5.71(d, J = 6.0 Hz, 2H), 3.00 (dd, J = 6.6, 7.0 Hz, 6H); MS (m/z; FAB): 756.79 (calculated for $[Ir(dfppy)_2(C_1\text{-bpy})]^+$; $C_{34}H_{24}F_4IrN_4$), 757 (experimentally obtained).

$[Ir(piq)_2(C_1\text{-bpy})]ClO_4$

^{1}H NMR (chloroform-*d,* 400 MHz, 25 °C): δ 8.97 (t, J = 5.53Hz, 2H), 8.70 (s, 2H), 8.28 (d, J = 8.00 Hz, 2H), 7.93 (d, J = 4.33 Hz, 2H), 7.79 (t, J = 4.40 Hz, 4H), 7.55 (d, J = 5.56 Hz, 2H), 7.44 (d, J = 6.87 Hz, 4H), 7.13 (m, J = 6.00 Hz, 4H), 6.93 (t, J = 8.44Hz, 2H), 6.32 (d, J = 6.71 Hz, 2H), 2.65 (s, 7.99 Hz, 6H); MS (m/z; FAB): 784.9 (calculated for $[Ir(piq)_2(C_1\text{-bpy})]^+$; $C_{42}H_{32}IrN_4$) 785 (experimentally obtained).

$[Ir(dfppy)_2(C_{12}\text{-bpy})]ClO_4$

^{1}H NMR (chloroform-*d*, 400 MHz, 25 °C): δ 9.45 (s, 2H), 8.32 (d, J = 8.8 Hz, 2H), 7.83 (dd, J = 6.0, 6.0 Hz, 2H), 7.73 (d, J = 6.0 Hz, 2H), 7.54 (d, J = 5.7 Hz, 2H), 7.25 (d, J = 5.7 Hz, 2H), 7.11 (dd, J = 6.0, 6.0 Hz, 2H), 6.57 (ddd, J = 9.3, 9.3, 2.5 Hz, 2H), 5.69 (dd, J = 6.0, 2.0 Hz, 2H), 2.97 (t, J = 7.7 Hz, 4H), 1,71 (tt, J = 7.7, 7.7 Hz, 4H), 1.42-1.20 (overlapped, 36H), 0.86 (t, J = 6.8 Hz, 6H); MS (m/z; FAB): 1068.1 (calculated for $[Ir(ppy)_2(C_{12}\text{-bpy})]^+$; $C_{56}H_{68}F_4IrN_4$), 1066 (experimentally obtained).

$[Ir(piq)_2(C_{12}\text{-bpy})]ClO_4$

^{1}H NMR (chloroform-*d,* 400 MHz, 25 °C): δ 8.91 (t, J = 5.43Hz, 2H), 8.72 (s, 2H), 8.25 (d, J = 7.99 Hz, 2H), 7.94 (t, J = 4.33 Hz, 2H), 7.79 (t, J = 4.39 Hz, 4H), 7.55 (t, J = 5.61 Hz, 2H), 7.44 (dd, J = 6.47 Hz, 4H), 7.15 (m, J = 5.92 Hz, 4H), 6.87 (t, J = 7.44Hz, 2H), 6.26 (d, J = 6.71 Hz, 2H), 2.91 (t, J = 7.99 Hz, 4H), 1.80(m, 4H),1.25 (s, 36H), 0.87 (t, J = 6.89 Hz, 6H) ; MS (m/z; FAB): 1096.7 (calculated for $[Ir(piq)_2(C_{12}\text{-bpy})]^+$; $C_{64}H_{76}IrN_4$) 1094 (experimentally obtained).

$[Ir(dfppy)_2(C_{19}\text{-bpy})]ClO_4$

^{1}H NMR (chloroform-*d*, 400 MHz, 25 °C): δ 9.40 (s, 2H), 8.28 (d, J = 8.8 Hz, 2H), 7.80 (dd, J = 6.0, 6.0 Hz, 2H), 7.70 (d, J = 6.0 Hz, 2H), 7.50 (d, J = 5.7 Hz, 2H), 7.21 (d, J = 5.7 Hz, 2H), 7.07 (dd, J = 6.0, 6.0 Hz, 2H), 6.53 (ddd, J = 9.3, 9.3, 2.5 Hz, 2H), 5.66 (dd, J = 6.0, 2.0 Hz, 2H), 2.99 (t, J = 7.7 Hz, 4H), 1,71 (tt, J = 7.7, 7.7 Hz, 4H), 1.42-1.20 (overlapped, 64H), 0.86 (t, J = 6.8 Hz, 6H); MS (m/z; FAB): 1261.7 (calculated for $[Ir(dfppy)_2(C19\text{-bpy})]^+$; $C_{70}H_{96}F_4IrN_4$), 1261 (experimentally obtained).

$[Ir(piq)_2(C_{19}\text{-bpy})]ClO_4$

^1H NMR (chloroform-*d,* 400 MHz, 25 °C): δ 8.91 (t, J = 5.43Hz, 2H), 8.73 (s, 2H), 8.27 (d, J = 7.99 Hz, 2H), 7.91 (t, J = 4.33 Hz, 2H), 7.78 (t, J = 4.39 Hz, 4H), 7.55 (t, J = 5.61 Hz, 2H), 7.44 (dd, J = 6.47 Hz, 4H), 7.11 (m, J = 5.92 Hz, 4H), 6.87 (t, J = 7.44Hz, 2H), 6.25 (d, J = 6.71 Hz, 2H), 2.90 (t, J = 7.99 Hz, 4H), 1.80(m, 4H),1.25 (s, 64H), 0.87 (t, J = 6.89 Hz, 6H) ; MS (m/z; FAB): 1273.7 (calculated for $[Ir(piq)_2(C_{19}\text{-bpy})]^+$; $C_{80}H_{104}IrN_4$) 1279 (experimentally obtained).

Examples of full charts of ^{1}H NMR spectra

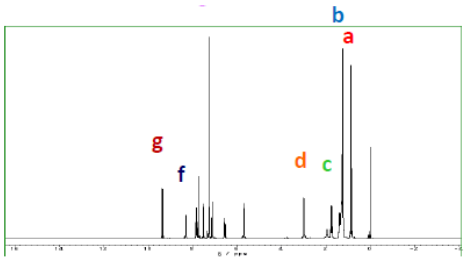

$[Ir(dfppy)_2(C_{12}\text{-bpy})]ClO_4$ in $CDCl_3$ (a, c, d and g, f are aliphatic and aromatic protons, respectively)

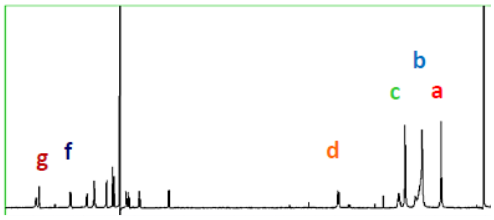

$[Ir(piq)_2(C_{12}\text{-bpy})]ClO_4$ in $CDCl_3$ (a, b, c, d and g, f are aliphatic and aromatic protons, respectively)

Examples of a full chart of ^{13}C NMR spectra

$[Ir(dfppy)_2(C_{19}\text{-bpy})]ClO_4$ in $CDCl_3$ (the region of aromatic carbons; 32 carbon atoms were identified; triplet peaks at $\delta = 78$ was due to the carbon of $CDCl_3$).

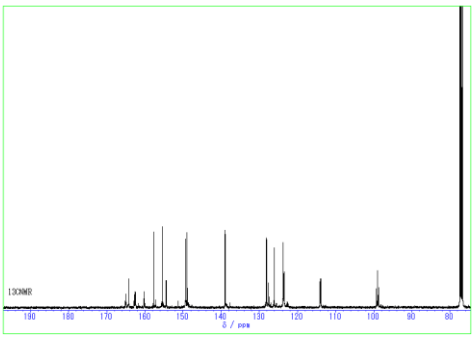

2. UV-spectra

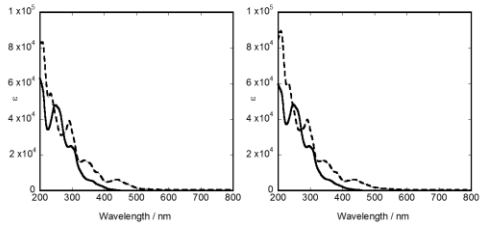

(C1) C_1-bpy (C12) C_{12}-bpy

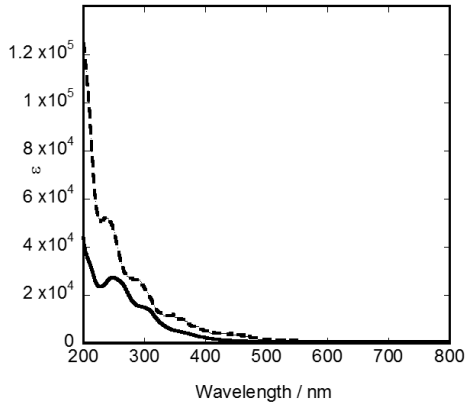

(C19) C_{19}-bpy

Figure S1. The UV-visible spectra of $[Ir(dfppy)_2(C_n\text{-bpy})]ClO_4$ (solid) and $[Ir(piq)_2(C_n\text{-bpy})]ClO_4$ (dotted) in methanol; C_n-bpy = (C1) C_1-bpy, (C12) C_{12}-bpy and (C19) C_{19}-bpy.

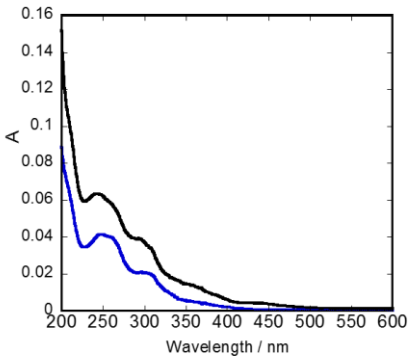

Figure S2. The UV-visible spectra of a suspension of SAP ($6x10^{-6}$ in CEC) adsorbing iridium(III) complexes: (blue) $[Ir(dfppy)_2(C_1\text{-bpy})]ClO_4$ ($9.3x10^{-7}$ M) was added and (black) $[Ir(piq)_2(C_1\text{-bpy})]ClO_4$ ($3.1x10^{-7}$ M) was added thereafter.

3. Chromatogram for optical resolution

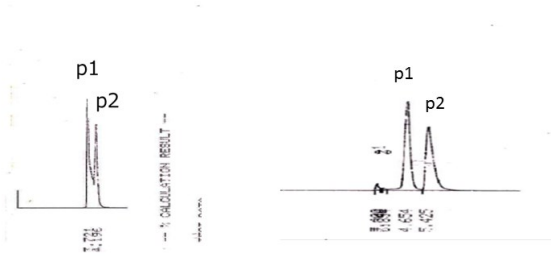

Figure S3. Chromatogram for resolving iridium(III) complexes: (left) $[Ir(dfppy)_2(C_1\text{-bpy})]ClO_4$;

The flow rate was 1.0 $mLmin^{-1}$ and the monitoring wavelength 400 nm.

(right) $[Ir(piq)_2(C_1\text{-bpy})]ClO_4$; The flow rate was 1.0 $mLmin^{-1}$ and the monitoring wavelength 500 nm.

The used column was a CHIRALPACK IA (Daicel, Japan). An eluting solvent was acetonitrile containing 0.1 % of diethylamine and trifluroroacetic acid.

4. **Stationary emission spectra**

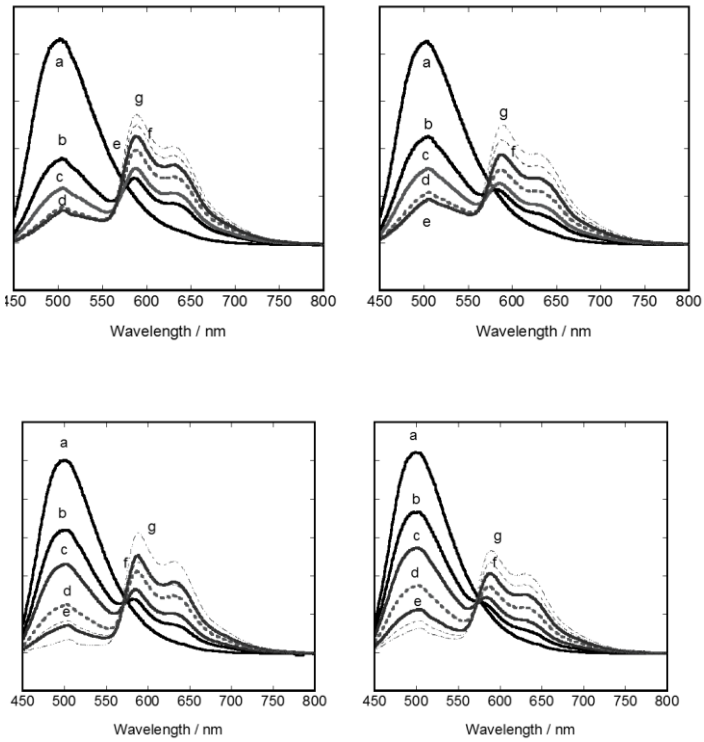

Figure S4. The change of the emission spectra of $[Ir(dfppy)_2(C_1\text{-bpy})]^+$ ions adsorbed by SAP, when a methanol solution of $[Ir(piq)_2(C_1\text{-bpy})]ClO_4$ was added. The used enantiomers were (left) Δ-$[Ir(dfppy)_2(C_1\text{-bpy})]^+$/Λ-$[Ir(piq)_2(C_1\text{-bpy})]^+$ and (right) Δ-$[Ir(dfppy)_2(C_1\text{-bpy})]^+$/Δ-$[Ir(piq)_2(C_1\text{-bpy})]^+$. The medium was 4:1 (v/v) warer/methanol. The concentration of SAP was (upper) $3.0\text{x}10^{-6}$ eqL^{-1} and (lower) $1.2\text{x}10^{-5}$ eqL^{-1} in terms of cation-exchange capacity and the loading of $[Ir(dfppy)_2(C_1\text{-bpy})]^+$ (upper) 60 % and (lower) 15 %, respectively. The loading of $[Ir(piq)_2(C_1\text{-bpy})]^+$ was (upper) (a) 0.0%, (b) 1.8%, (c) 3.8%, (d)7.4%, (e) 11.2%, (f) 15.0% and (g) 18.4% and (lower) (a) 0.0%, (b) 0.45%, (c) 0.95%, (d) 1.8%, (e) 2.8 %, (f) 3.7 % and (g) 4.6 %, respectively.

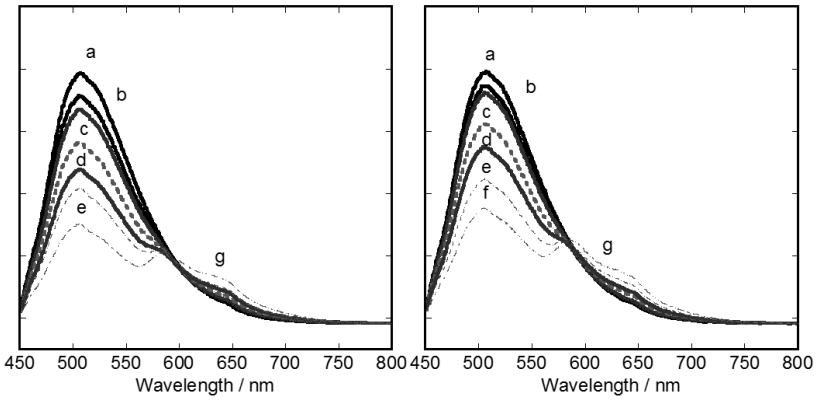

Figure S5. The change of the emission spectra of $[Ir(dfppy)_2(C_{12}\text{-bpy})]^+$ ions adsorbed by SAP, when a methanol solution of $[Ir(piq)_2(C_{12}\text{-bpy})]ClO_4$ was added. The used enantiomers were (left) Δ-$[Ir(dfppy)_2(C_{12}\text{-bpy})]^+$/Λ-$[Ir(piq)_2(C_{12}\text{-bpy})]^+$ and (right) Δ-$[Ir(dfppy)_2(C_{12}\text{-bpy})]^+$/Δ-$[Ir(piq)_2(C_{12}\text{-bpy})]^+$. The medium was 4:1 (v/v) water/methanol. The concentration of SAP was $3.0\text{x}10^{-6}$ eqL^{-1} in terms of cation-exchange capacity and the loading of $[Ir(dfppy)_2(C_1\text{-bpy})]^+$ 60%. The loading of $[Ir(piq)_2L]^+$ was (a) 0.0%, (b) 2.0%, (c) 4.0%, (d)7.9%, (e) 11.8%, (f) 15.7% and (g) 19.5%, respectively.

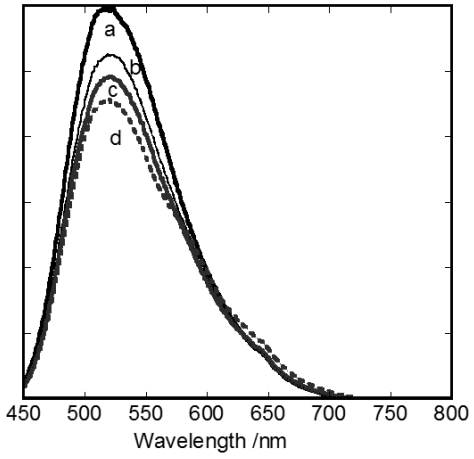

Figure S6. The change of the emission spectra of $[Ir(dfppy)_2(C_{19}\text{-bpy})]^+$ ions adsorbed by SAP, when a methanol solution of $[Ir(piq)_2(C_{19}\text{-bpy})]ClO_4$ was added. The concentration of SAP was $3.0\text{x}10^{-6}$ eqL^{-1} in terms of cation-exchange capacity and the loading of $[Ir(dfppy)_2(C_1\text{-bpy})]^+$ 60%. The loading of $[Ir(piq)_2L]^+$ was (a) 0.0%, (b) 5.9%, (c) 11.9%, and (d)23.6%, respectively.

5. Dynamic emission properties

Table S1. The lifetime analyses of the emission decay at 490 nm according to eq. (3) in the text

SAP	1.2×10^{-5}M	1.2×10^{-5}M	6×10^{-6} M	6×10^{-6}M
PIQ [M]	τ_{fast} / μs	τ_{slow} / μs	τ_{fast} / μs	τ_{slow} / μs
0	0.315	0.713	0.302	0.745
8.8×10^{-8}	0.188	0.604	0.076	0.490
1.7×10^{-7}	0.120	0.513	0.059	0.414
3.5×10^{-7}	0.089	0.442	0.045	0.379
5.3×10^{-7}	0.063	0.380	0.039	0.328
7.1×10^{-7}	0.058	0.385	0.039	0.344
8.8×10^{-7}	0.043	0.344	0.039	0.369

6. Calculation of spectral overlap integral (J) and Förster radius (R_0)

The rate constant of Förster-type energy transfer (k_{ET}) is expressed by the following equation:

$$k_{ET} = \frac{9000\ Ln10\ \ k^2\ \phi}{128\pi^5 n^4 N \tau_D R^6} J(\lambda) \qquad \text{(S1)},$$

in which τ_D, R and J (λ) denote the excited life time of a donor in the absence of an acceptor, the donor/acceptor distance and the spectral overlap integral, respectively. R_o (Förster radius) and J (λ) are given by equations (S2) and (S3), respectively:

$$R_0 = 9.78 \times 10^{-5} (\kappa^2 \phi n^{-4} J(\lambda))^{\frac{1}{6}}$$

(in cm) (S2).

$$J(\lambda) = \frac{\int F_d(\lambda)\varepsilon(\lambda)\lambda^4 d\lambda}{\int F_d(\lambda) d\lambda} \qquad \text{(S3)}$$

As for other parameters in equations (S2) and (S3), κ is the orientation factor, ϕ the quantum yield of donor, n the refractive index of the medium, N the Avogadro constant, λ the wavelength, ε_a the extinction coefficient of the acceptor and F_d the normalized emission intensity of the donor. η_{ET} denotes the energy transfer efficiency and k_{NR} represents the decay constant in the absence of an acceptor. Assuming $\kappa^2 = 2/3$ (random orientation), n = 1.3 and ϕ=0.14, J (λ) was calculated to be 1.14 x 10^{-14} $M^{-1}cm^3$ from the emission and absorption spectra of the present donor-acceptor pairs. R_o was obtained to be 2.6 nm for a donor/acceptor pair. For a donor/donor pair, J (λ) was calculated to be 2.68 x 10^{-15} $M^{-1}cm^3$ from the emission and absorption spectra of the present excited donor-donor pairs. R_o was obtained to be 2.0 nm.

7. XRD patterns of ion-exchange adducts

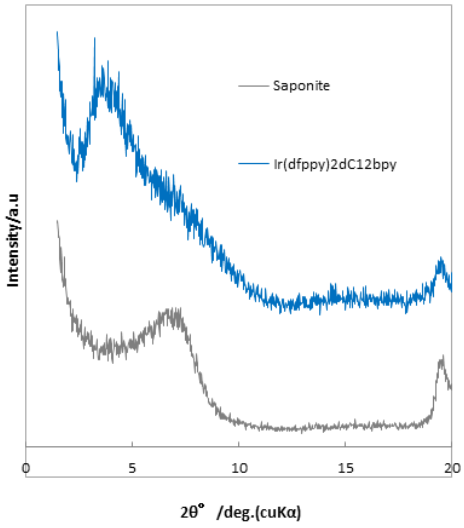

Figure S7. The XRD patterns of SAP: (black) the original sample with the basal spacing (d) of 2.0 nm and (blue) the samples having adsorbed $[Ir(dfppy)_2(C_{12}\text{-bpy})]^+$ to c.a. 90 % of CEC with d = 2.2 nm.